

Hysteresis in an Electrochemical System: Br Electrodeposition on Ag(100)

S.J. Mitchell, G. Brown, P.A. Rikvold

Center for Materials Research and Technology,

Department of Physics, and

School of Computational Science and Information Technology,

Florida State University, Tallahassee, Florida 32306-4351, USA

November 14, 2018

Abstract

We examine hysteresis in cyclic voltammetry of Br electrosorption onto single-crystal Ag(100) by dynamic Monte Carlo simulations. At room temperature, this system displays a second-order phase transition from a low-coverage disordered phase to a doubly degenerate $c(2 \times 2)$ phase. The electrochemical potential is ramped back and forth across the phase transition, linearly in time, and the phase lag between the response of the adlayer and the potential is observed to depend on the sweep rate. The hysteresis in this system is caused by slow ordering/disordering kinetics and critical slowing-down.

Hysteresis is a widely occurring phenomenon in which a system is driven too fast to remain near equilibrium, resulting in a phase lag between the response and the oscillating driving force. Some common examples include magnetic systems in oscillating external fields [1, 2], electrochemical adsorption in an oscillating electrochemical potential [3, 4, 5], and nonlinear media under oscillating stress. As an example of hysteresis at a second-order phase transition, we here present preliminary results of dynamic Monte Carlo simulations of the electrosorption of Br onto single-crystal Ag(100) under a time-varying electrochemical potential, known as cyclic voltammetry (CV) in the electrochemical literature.

In equilibrium at room temperature, this system displays a second-order phase transition in the Ising universality class from a low-coverage disordered phase at more negative potentials to a doubly degenerate $c(2 \times 2)$ ordered phase at more positive potentials [3]. As the system is driven back and forth across this phase transition, hysteresis is observed [3]. Unlike magnetic systems [1, 2] and some electrochemical systems [4], in which hysteresis is usually associated with metastable decay near a first-order phase transition [1, 4], hysteresis in the Br/Ag(100) system is associated with kinetic limitations to the phase ordering/disordering processes and critical slowing-down in the neighborhood of the second-order transition.

The model and the dynamic Monte Carlo algorithm are discussed in detail in Ref. [5] and are only briefly summarized here. *In-situ* X-ray scattering indicates that the Br adlayer is commensurate with the square Ag(100) lattice, with Br adsorbing at the four-fold hollow sites between the Ag atoms [3]. This arrangement suggests a lattice-gas treatment of the adlayer. We used an $L \times L$ square lattice of adsorption sites with periodic boundary conditions. The grand-canonical lattice-gas Hamiltonian is [4, 5, 6]

$$\mathcal{H} = - \sum_{i < j} \phi_{ij} c_i c_j - \mu \sum_{i=1}^{L^2} c_i , \quad (1)$$

where i and j denote sites on the lattice, c_i denotes the occupation of site i (0 for empty and 1 for occupied), $\sum_{i < j}$ denotes a sum over all pairs of sites on the lattice, ϕ_{ij} denotes the lateral interaction

energy of the pair (i, j) , and μ is the electrochemical potential. The sign convention is such that $\phi_{ij} < 0$ denotes a repulsive interaction, and $\mu > 0$ favors adsorption.

The interactions are quite adequately described with a nearest-neighbor excluded-volume interaction (infinite repulsion) caused by the large ionic radius of Br, plus a long-range dipole-dipole repulsion [5, 6]. The lateral pair interactions are [5]

$$\phi(r) = \begin{cases} -\infty & r = 1 \\ 2^{3/2}\phi_{\text{nnn}}/r^3 & \sqrt{2} \leq r \leq 5, \\ 0 & r > 5 \end{cases} \quad (2)$$

where r is the separation of an interacting Br pair within the adlayer, measured in units of the Ag(100) lattice spacing, and ϕ_{nnn} is the value of the repulsion between next-nearest neighbors. The repulsion was truncated to simplify computation. We found $\phi_{\text{nnn}} = -26$ meV/pair by fitting equilibrium simulation isotherms to experimental adsorption isotherms [5].

To simulate the microscopic dynamics, we used a thermally activated stochastic barrier-hopping scheme, which include adsorption, desorption, and nearest- and next-nearest neighbor diffusion. These processes were represented by transitions between initial and final lattice-gas states, I and F , respectively, through intermediate transition states of higher energy. These intermediate states, T_λ , cannot be represented by lattice-gas configurations, and the subscript λ indicates the process (adsorption/desorption, *etc.*) which relates I to F . The energies of these transition states were approximated as [4, 5]

$$U_{T_\lambda} = (U_I + U_F)/2 + \Delta_\lambda, \quad (3)$$

where U_{T_λ} , U_I , and U_F are the energies of the states T_λ , I , and F , respectively, and Δ_λ is the barrier associated with the process λ .

We approximated the probability $R(F|I)$ of making a transition from I to F during one time step by an Arrhenius rate [4, 5]

$$R(F|I) = \nu \exp\left(-\frac{U_{T_\lambda} - U_I}{k_B T}\right) = \nu \exp\left(-\frac{\Delta_\lambda}{k_B T}\right) \exp\left(-\frac{U_F - U_I}{2k_B T}\right), \quad (4)$$

where k_B is Boltzmann's constant, T is the temperature, and ν is a dimensionless attempt frequency which sets the overall time scale of the simulation. For all simulations discussed here, the temperature was 290 K, corresponding to $k_B T = 25$ meV. The nearest-neighbor diffusion barrier was $\Delta_{\text{nn}} = 100$ meV and the next-nearest neighbor diffusion barrier was $\Delta_{\text{nnn}} = 200$ meV, consistent with *ab initio* calculations [7]. The adsorption/desorption barrier was $\Delta_a = 300$ meV, and we used $\nu = 1$ [5]. Time was measured in Monte Carlo steps per site (MCSS).

The nearest-neighbor excluded-volume interaction gives rise to two degenerate $c(2 \times 2)$ ordered phases, each occupying one of two sublattices, A and B . The sublattice coverage, Θ_A , is the fraction of occupied sites on sublattice A , and analogously for Θ_B . There are two observables of interest: the total Br coverage, $\Theta = (\Theta_A + \Theta_B)/2$, and the staggered coverage $\Theta_S = \Theta_A - \Theta_B$, which is the $c(2 \times 2)$ order parameter. Figure 1 shows equilibrium Θ and $|\Theta_S|$ isotherms obtained by Monte Carlo simulation using a single-site Metropolis algorithm [5]. The transition occurs at a critical electrochemical potential, $\mu_c = 180 \pm 5$ meV/particle [5].

Although hysteresis studies in magnetic systems usually use sinusoidally varying fields, CV experiments mostly use linearly ramped electrochemical potentials. For the hysteresis (dynamic CV) simulations, the Br/Ag(100) system was first equilibrated in the low-coverage phase at $\mu_1 \ll \mu_c$. Then μ was ramped linearly in time up to $\mu_2 \gg \mu_c$ at a rate of ρ meV/MCSS. After reaching μ_2 , the potential was ramped back down to μ_1 at the same rate [5]. Because of the long simulation times, only a single cycle was simulated for each value of ρ .

Figure 2 shows hysteresis loops, Θ vs. μ , which are analogous to magnetization vs. field plots commonly shown for hysteresis in magnets [1, 2]. However, for CVs, $d\Theta/dt$ vs. μ is usually shown, since $d\Theta/dt$ is directly measurable as proportional to the electric current through the electrochemical cell, Fig. 3. This figure also shows a quasi-equilibrium CV, obtained by differentiating the equilibrium coverage isotherm in Fig. 1 with respect to μ . In the limit of zero sweep rate, the dynamic CVs should have the same shape and μ placement as the quasi-equilibrium CV for the same system size.

The asymmetry between the positive-going scans (positive $d\Theta/dt$) and the negative-going scans is caused by the difference in the ordering (positive scan) and disordering (negative scan) dynamics. In the limit of zero sweep rate, positive and negative scans would be symmetric. Figure 4 shows the height, $(d\Theta/dt)_{\max}$, and position, μ_p , of the sharp peak in the positive-going scans vs. ρ .

In conclusion, we have studied the hysteresis of the Br/Ag(100) adlayer by dynamic Monte Carlo simulation. We observed asymmetry between the positive and negative-going scans, which is expected to vanish in the limit of zero sweep rate. We also observed a power-law relationship between $\rho^{-1}(d\Theta/dt)_{\max}$ and ρ with a measured effective exponent of ≈ -0.08 . Future work will include slower sweep rates to test these observed behaviors.

This research was supported in part by the National Science Foundation through Grants No. DMR-9634873 and DMR-9981815, and by Florida State University through the Center for Materials Research and Technology, the Supercomputer Computations Research Institute (US Department of Energy Contract No. DE-FC05-85ER25000), and the School of Computational Science and Information Technology.

References

- [1] S. W. Sides, P. A. Rikvold, and M. A. Novotny, Phys. Rev. E **59** 2710 (1999).
- [2] P. A. Rikvold, G. Korniss, C. J. White, M. A. Novotny, and S. W. Sides, in *Computer Simulation Studies in Condensed-Matter Physics XII*, edited by D. P. Landau, S. P. Lewis, and H.-B. Schüttler, Springer Proceedings in Physics **85**, (Springer-Verlag, Berlin, 2000), and refs. cited therein.
- [3] B. M. Ocko, J. X. Wang, and T. Wandlowski, Phys. Rev. Lett. **79** 1511 (1997).
- [4] G. Brown, P. A. Rikvold, S. J. Mitchell, and M. A. Novotny, in *Interfacial Electrochemistry: Theory, Experiment, and Applications*, edited by A. Wieckowski (Marcel Dekker, New York, 1999).
- [5] S. J. Mitchell, P. A. Rikvold, and G. Brown, submitted to Surf. Sci.
- [6] M. T. M. Koper, J. Electroanal. Chem. **45**, 189 (1998).
- [7] A. Ignaczak and J. A. N. F. Gomes, J. Electroanal. Chem. **420** 71 (1997).

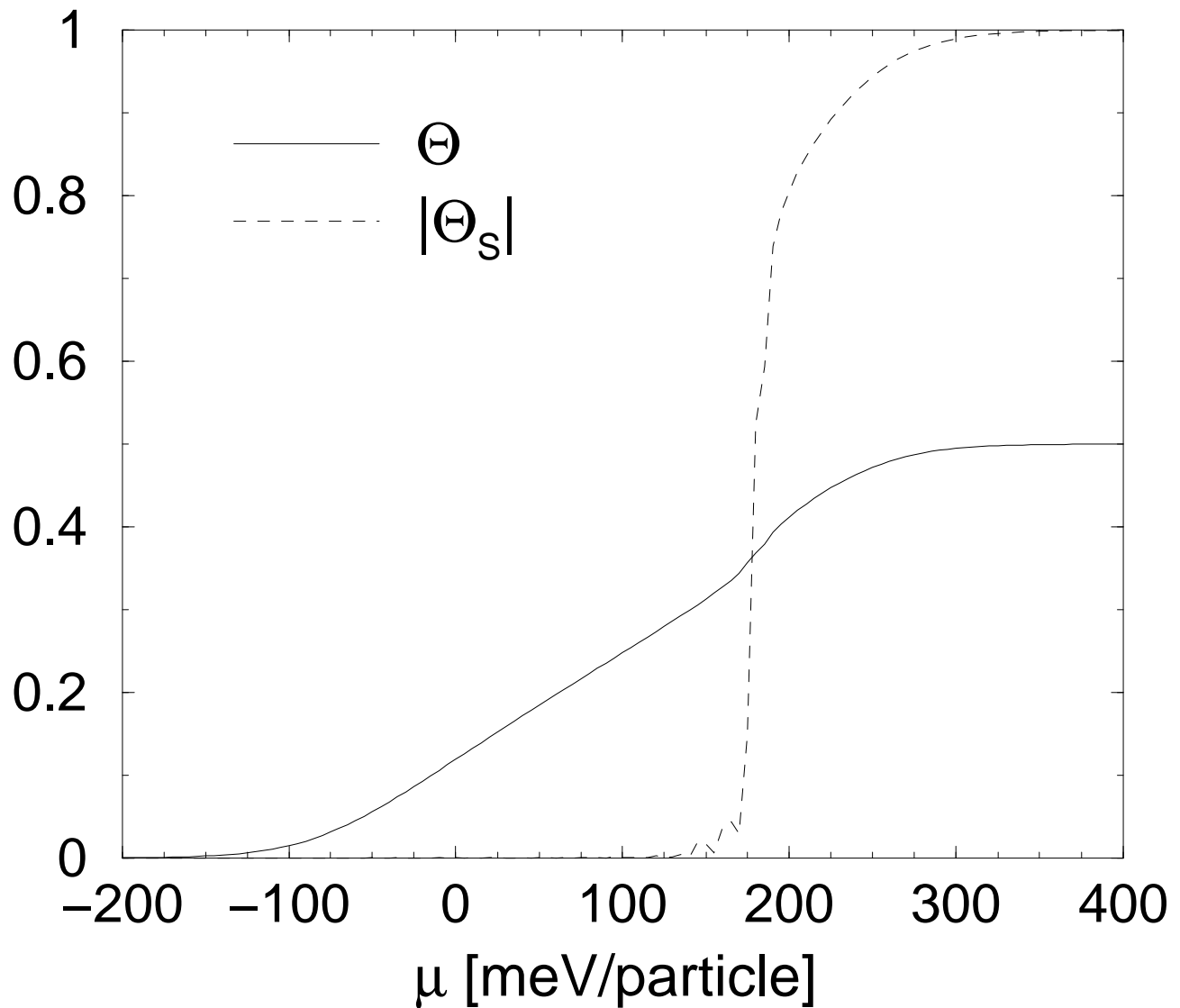


Figure 1: Equilibrium Monte Carlo isotherms for $L=32$. A second-order phase transition between a low-coverage disordered phase and a $c(2 \times 2)$ phase with $\Theta=1/2$ is observed at μ_c . The isotherm was generated from 10,000 independent samples for each value of μ .

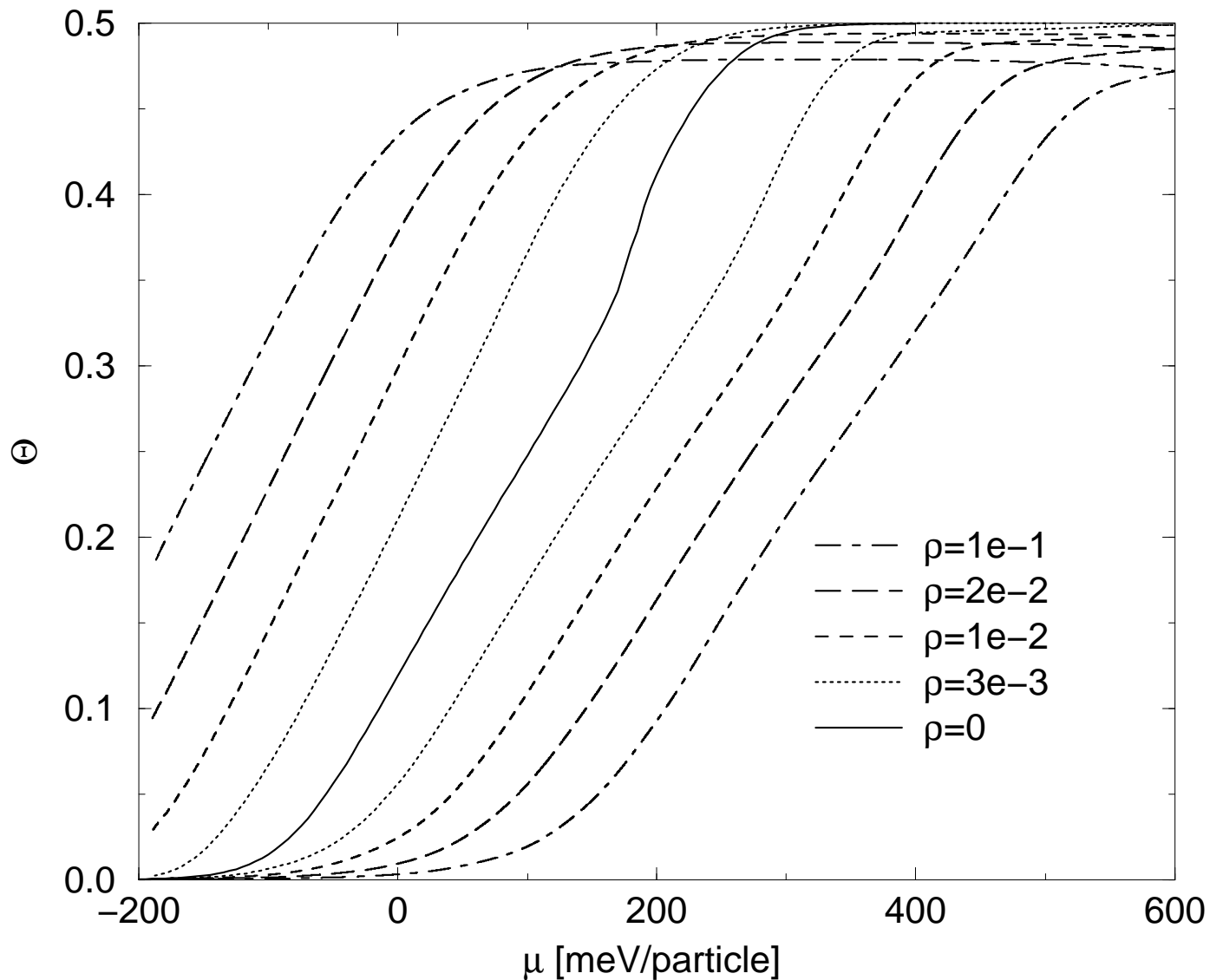
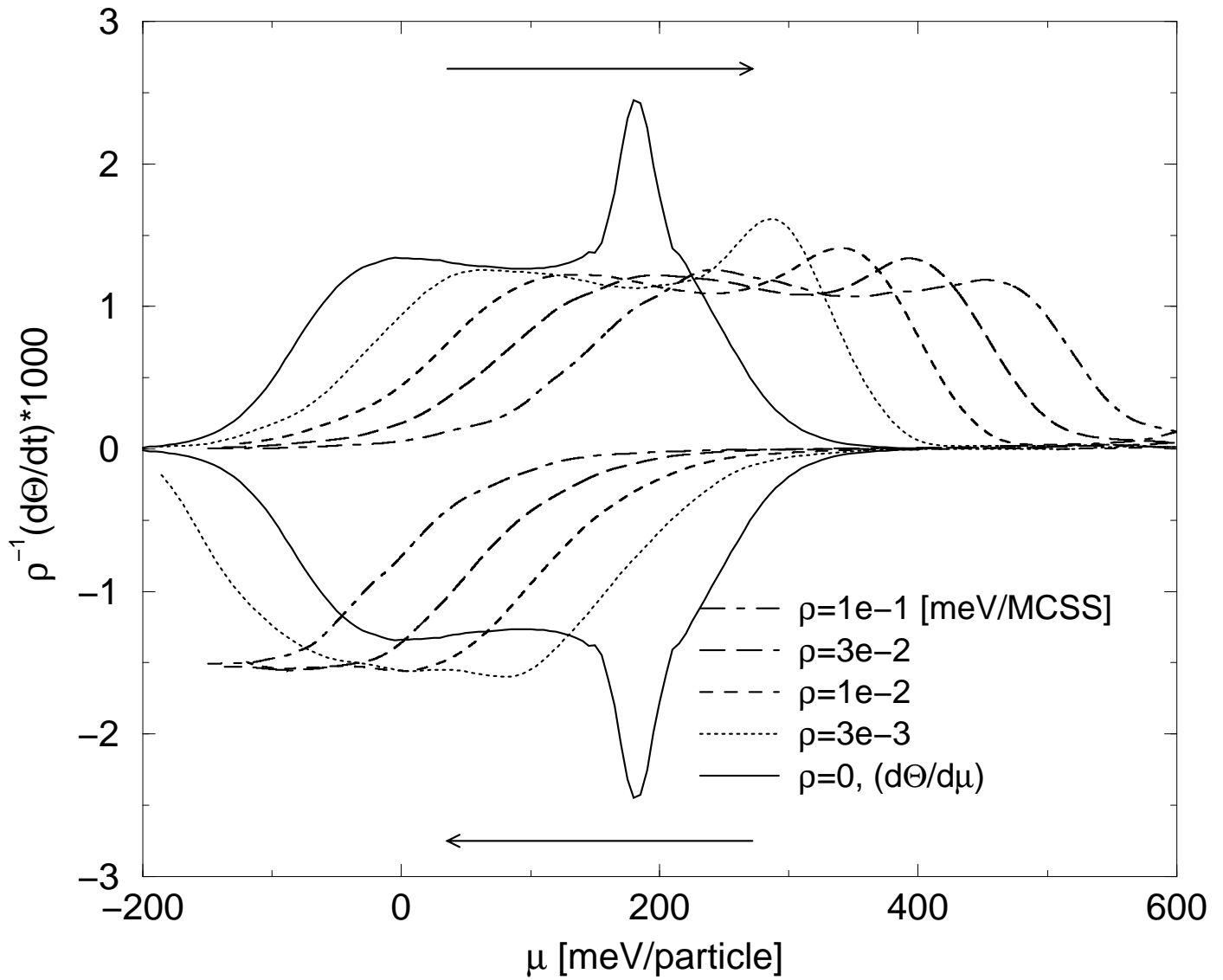


Figure 2: Hysteresis loops at various sweep rates ρ . All curves show Θ vs. μ for $L=256$, except for the solid curve, $\rho=0$, which shows equilibrium for $L=32$, Fig. 1.



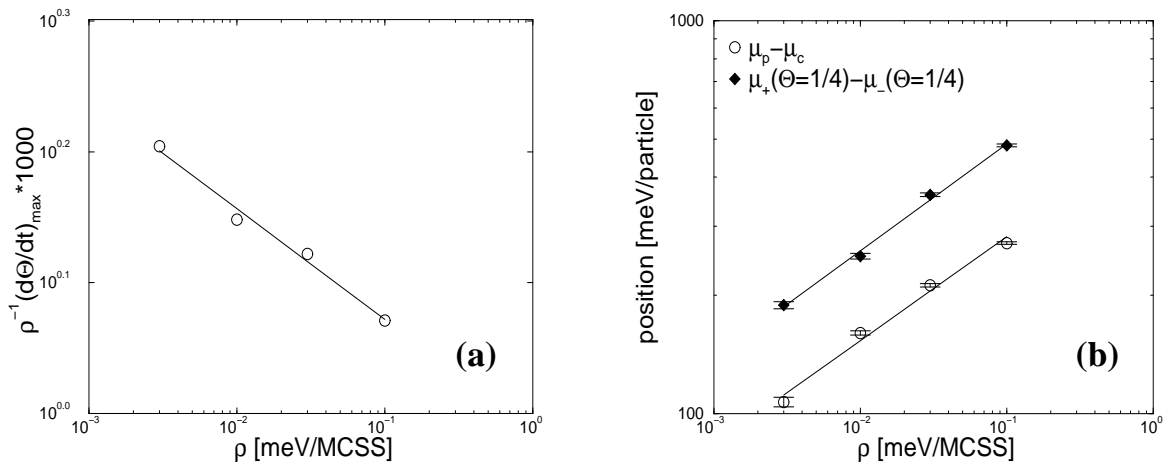


Figure 4: CV peak position and height vs. sweep rate. **(a)** shows the positive-going peak height with errors much smaller than the symbol size. **(b)** shows the peak displacement from μ_c , $\mu_p - \mu_c$, and the distance in μ between $\Theta=1/4$ in the positive-going and negative-going scans in Fig. 2.